

See discussions, stats, and author profiles for this publication at: <http://www.researchgate.net/publication/280654549>

ANALYSIS OF SUB-MESOSCALE EDDIES IN THE BALTIC SEA BASED ON SAR IMAGERY AND MODEL WIND DATA

CONFERENCE PAPER · JULY 2015

READS

20

2 AUTHORS:



[Svetlana Karimova](#)

Helmholtz-Zentrum Geesthacht

15 PUBLICATIONS 34 CITATIONS

[SEE PROFILE](#)



[Martin Gade](#)

University of Hamburg

111 PUBLICATIONS 788 CITATIONS

[SEE PROFILE](#)

ANALYSIS OF SUB-MESOSCALE EDDIES IN THE BALTIC SEA BASED ON SAR IMAGERY AND MODEL WIND DATA

Svetlana Karimova¹ and Martin Gade²

¹ Helmholtz-Zentrum Geesthacht (HZG), Institut für Küstenforschung
Max-Planck-Str. 1, Geesthacht, 21502, Germany
Email: svetlana.karimova@hzg.de

² Universität Hamburg (UHH), Institut für Meereskunde, Hamburg, Germany

ABSTRACT

We discuss the spatio-temporal distribution of sub-mesoscale eddies seen in synthetic aperture radar (SAR) imagery of the Baltic Sea. Analyzing about 1250 Envisat Advanced SAR (ASAR) images acquired between 2009 and 2011 almost 7000 sub-mesoscale eddies were discovered. Since the visibility of vortical structures in SAR imagery significantly depends on the near-surface wind speed, wind data from a numerical model of the Baltic Sea were additionally used to improve our eddy statistics. Within the method proposed herein only those parts of SAR images are considered for the calculation of eddy statistics, which were acquired when the wind speed conditions were favorable for eddy manifestations. As a result, and despite the fact that eddies were generally observed all over the Baltic Sea, we show that the south-western part of the Baltic Sea seems to have especially high sub-mesoscale eddy activity.

Index Terms— SAR, sub-mesoscale eddies, spiral eddies, eddy statistics, Baltic Sea

1. INTRODUCTION

Satellite synthetic aperture radar (SAR) imagery provides the unique opportunity to study sub-mesoscale surface dynamics in the World's oceans. Due to the high spatial resolution of such imagery eddies with a diameter as small as 1 km (and for the latest sensors even less) can be identified. Therefore, the analysis of a long-term time series of SAR images can provide a good insight into the sub-mesoscale eddy activity within a certain region [3-4, 8-10]. Nevertheless, the statistics retrieved can be significantly biased due to a strong dependence of eddy manifestations on the near-surface wind speed. The aim of the present study is therefore to provide a methodology to exclude the effect of seasonal and spatial wind-speed variability on eddy statistics based on SAR imagery.

2. DATA AND METHODS

In the present study about 1250 Envisat Advanced SAR (ASAR) Wide Swath (WS) images obtained in 2009-2011 over different parts of the Baltic Sea were used. The pixel size of such images is of 75 m. The maximum coverage (up to about 500 images) by SAR imagery was found in the northern Baltic Proper (Gotland Sea) and in the adjacent areas (southern Bothnian Sea, Åland Sea, Gulf of Riga, and western Gulf of Finland).

In SAR images water circulation features can be manifested through suppression of short wind waves by natural films, wave/current interactions, and a varying wind field, resulting from changes of the atmospheric boundary layer across an oceanic temperature front [1, 3-5].

At moderate wind speeds (up to about 5 m/s) eddies usually appear in SAR images due to the presence of natural films on the sea surface [5], which dampen capillary and short gravity waves. Surfactant films are entrained by the orbital motion of the eddies, which thereby are manifesting in radar images [1, 6]. Since slick streaks in SAR images look dark, for shortness sake, eddies visualized due to slicks are hereinafter referred to as “black” eddies.

At higher wind speeds (exceeding 5-7 m/s) eddies appear in SAR imagery as a result of wave/current interactions in zones of current shear and look like bright curved lines [4, 7]. Because of the enhanced radar backscattering within such signatures, eddies of this type are hereinafter referred to as “white” eddies. In Fig. 1, examples of well-visualized “black” and “white” eddies detected in the eastern Baltic Sea are presented. These Envisat ASAR WS images were obtained on 22.06.2009 08:47 UTC (a) and 07.05.2007 09:06 UTC (b), respectively.

The hourly data on near-surface wind speed for 2009-2011 with a spatial resolution of 5 km (253 × 250 grid cells for the domain used) were provided by the German Weather Service (Deutscher Wetterdienst, DWD) from their meteorological forecast model.

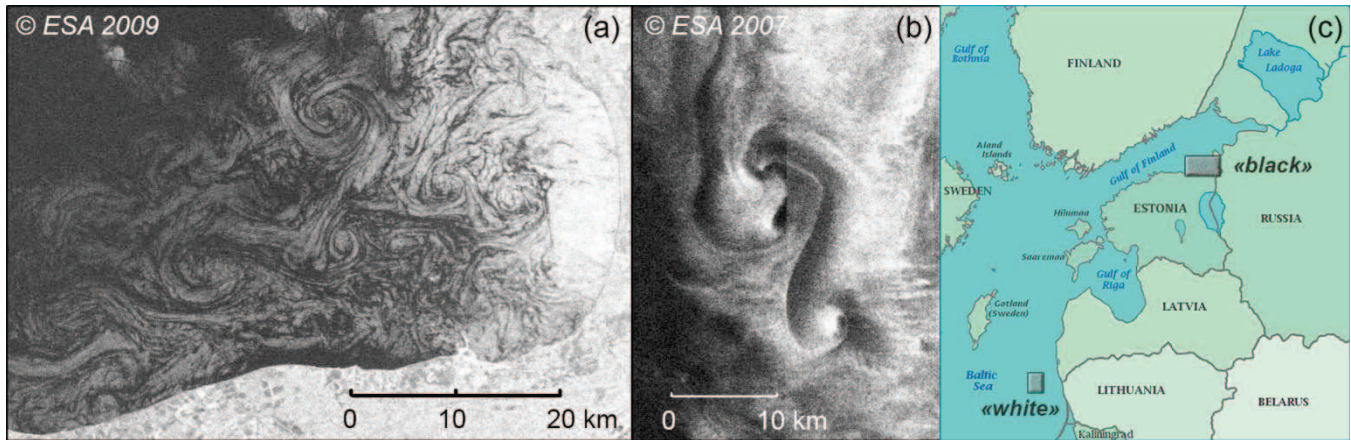


Fig. 1. (a) “Black” eddies; (b) “white” eddies; (c) geographical location of the fragments shown.

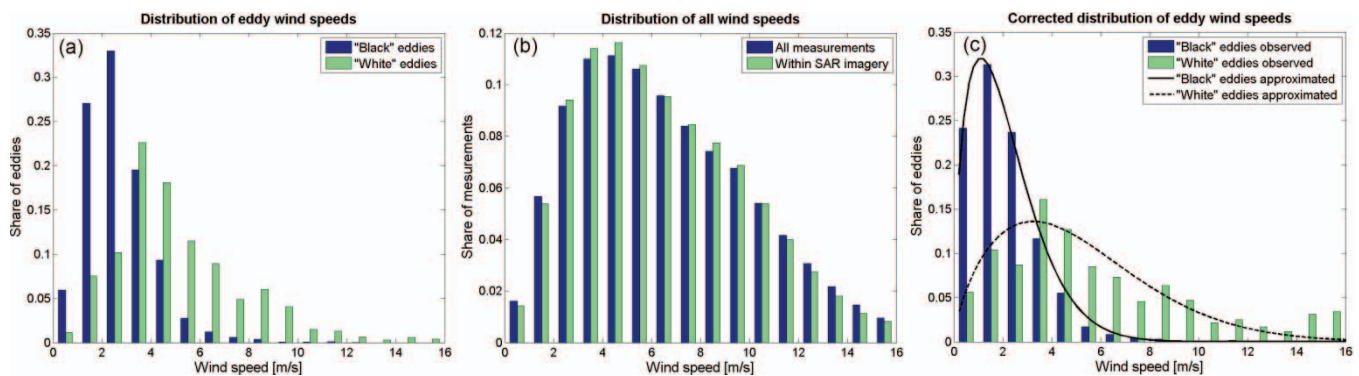


Fig. 2. (a) Distribution of wind speeds at which “black” and “white” eddies were found; (b) general distribution of wind speeds over the Baltic Sea in 2009-2011; (c) normalized eddy visibility as ratio of the distributions in (a) and the general wind speed distribution during SAR acquisitions.

3. ALGORITHM APPLIED AND THE RESULTS OBTAINED

3.1. Preliminary procession

As the first step, the SAR imagery described above was visually inspected and the geographical coordinates of the eddy manifestations and their diameters were fixed using the BEAM VISAT software. As eddy manifestations, we considered fully or partly visible spiral structures or circular areas with enhanced roughness (“white” eddies). The general characteristics of the eddies revealed are as follow:

- About 32 % of the analyzed 1250 images contained eddy manifestations.
- A total of 6880 eddy manifestations were detected.
- Among them there were 5670 “black” and 1208 “white” ones (17.6 % of “white” eddies).
- About 95 % of the eddies had diameters between 1 km and 15 km.
- About 90 % of the eddies discovered were cyclonically rotating.

3.2. Defining wind speed limits

The aim of this subsection is to define the wind speed ranges at which eddies can be detected in the analyzed SAR imagery. In order to do so, for every eddy detected the corresponding wind speed (from the closest in space and time model grid cell) was retrieved from model data.

The resulting distributions of wind speeds found to be in correspondence with “black” and “white” eddy manifestations are shown in Fig. 2a. The total distribution of the wind speeds over the entire Baltic Sea, as well as the wind-speed distribution for the times and places of SAR image acquisitions, are shown in Fig. 2b. Finally, Fig. 2c shows the “normalized eddy visibility”, calculated as the ratio of the respective distributions of the “black” and “white” eddies (Fig. 2a) and the general wind-speed distribution (Fig. 2b). The resulting histograms (Fig. 2c) reflect the general distribution of wind-speeds at which “black” and “white” eddies can be seen in SAR imagery, independent of the specific wind speed conditions in the Baltic Sea.

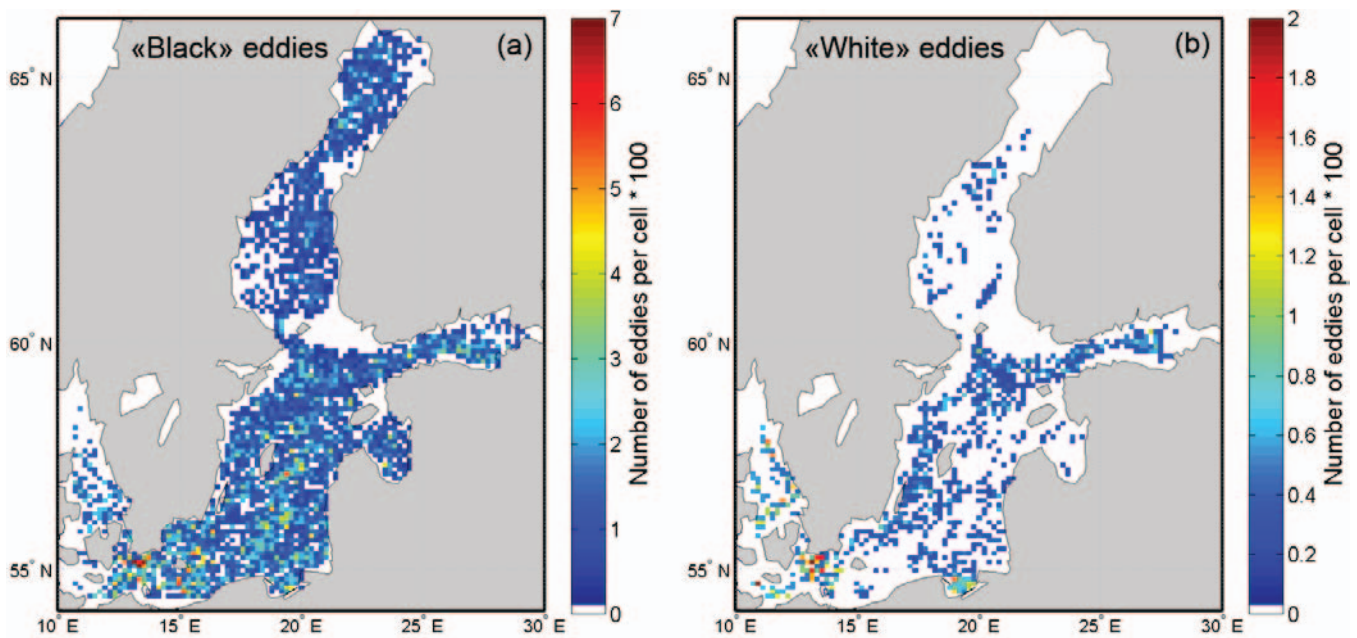


Fig. 3. Density of (a) “black” and (b) “white” eddies normalized by the corrected SAR coverage density.

In order to allow for a more precise definition of the upper and lower wind-speed limits for the detection of “black” and “white” eddies, the best-fit Weibull distributions were added to the columns in Fig. 2c. To quantify the wind-speed limits for the visualization of both eddy types we used the 2.5 % and 97.5 % quantiles of the calculated (best-fit) distributions, i.e., we calculated the wind-speed ranges, in which 95 % of the eddies were manifesting in the SAR imagery. For “black” eddies, this is $0.2 \text{ m}\cdot\text{s}^{-1}$ to $5.6 \text{ m}\cdot\text{s}^{-1}$, and for “white eddies” it is $0.6 \text{ m}\cdot\text{s}^{-1}$ to $12.5 \text{ m}\cdot\text{s}^{-1}$. These limits were used for our corrected statistics presented below.

3.3. Spatial distribution of eddies

In order to reveal the peculiarities of the spatial distribution of eddies, the eddy density (i.e., the number of eddies per pixel) and coverage density (i.e., the coverage by SAR images) fields were calculated using a regular grid of $0.2^\circ \times 0.1^\circ$. While calculating the coverage density the areas with “improper” wind speeds were excluded. The obtained fields were used to get the corrected eddy density schemes, namely for every pixel the number of eddies discovered was divided by the number of covering images and for convenience multiplied by 100. These normalized eddy density fields are provided in Fig. 3.

One can observe that the density field for “black” eddies (Fig. 3a) exhibits higher values in the south-western part of the Baltic Sea. Comparison with location of thermal fronts retrieved from sea surface temperature maps (not shown here) allowed as to suggest that high eddy activity in this area can be caused by the high persistence of thermal fronts and consequent frontal hydrodynamic instability.

As for “white” eddies, the highest densities were found in the southernmost part of the Baltic Sea, to the west from the island of Bornholm (Arkona Sea), in the Bay of Gdansk, and in the Kattegat Strait (Fig. 3b). A comparison with distribution of thermal fronts and mean surface currents revealed that “white” eddies tend to be located in the areas with both sharp thermal fronts and strong surface currents.

3.4. Temporal distribution of eddies

In order to characterize the temporal (e.g., seasonal) variability of eddy appearances in SAR imagery, the daily numbers of the detected “black” and “white” eddies were calculated and then normalized by the sea surface area covered daily by the SAR images under favorable wind conditions. The average daily number of “black” and “white” eddies per 100 km^2 of sea area is shown in Fig. 4. In these plots, the dots represent the actual values obtained, while the solid line is a result of smoothing performed by the moving average algorithm with width 30 days.

We note that the number of detected “black” eddies (Fig. 4) significantly depends on the season: the highest values of the average number of “black” eddies were observed in the period from summer to mid-autumn. The strong eddy activity during the warm period of the year can be explained by a generally higher availability of surface-active material in the entire area. Moreover, overall moderate wind speeds and shallow thermocline depths, both prevailing during this time of the year, allow for a relaxation of surface waters after stronger atmospheric and hydrodynamical forcing and thus support the formation and evolution of eddies.

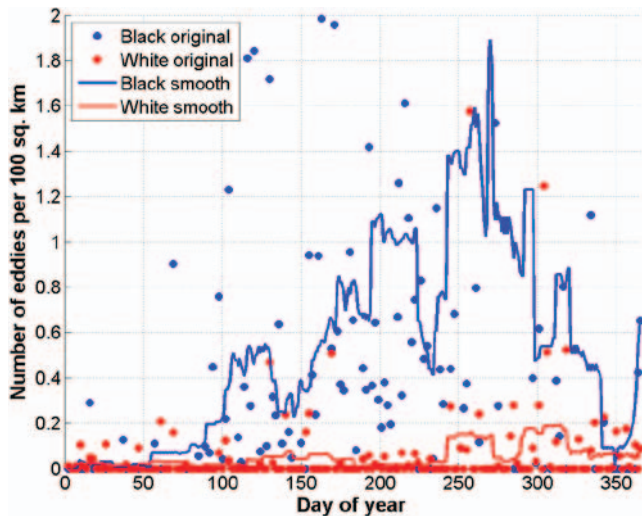


Fig. 4. Daily average number of “black” and “white” eddies per 100 km² of the sea surface covered by SAR imagery under proper wind conditions.

The highest values of the average number of “white” eddies were found from mid-October to mid-November (Fig. 4). Apparently during this time of the year, favorable combinations of surface currents and near-wind surface wind speed were encountered, resulting in a higher occurrence of “white” eddies in SAR imagery. In contrast, lowest numbers of “white” eddies were observed in July – August, which corresponds to the time of lowest average wind speeds over the Baltic Sea.

4. CONCLUSIONS

In the present study a method for improving eddy statistics retrieved from SAR imagery is proposed. The method is based on the idea that only those parts of SAR images are used for our eddy statistics, where the wind conditions were favorable for eddy visualization on SAR imagery.

The method was applied to 6880 eddy manifestations found in about 1250 Envisat ASAR images of the Baltic Sea. This allowed us, for the first time, (i) to statistically retrieve the limits of the eddy visibility in SAR imagery, and (ii) to obtain wind-corrected spatial and temporal statistics of sub-mesoscale eddies in the Baltic Sea. We found that 95 % of the “black” eddies were found at the wind speeds of up to 5.6 m·s⁻¹, while the upper wind speed limit for “white” eddies was found to be 12.5 m·s⁻¹.

“Black eddies” were most frequently found in the south-western Baltic Sea, presumably due to a high persistence of thermal fronts in that area. The normalized density of “white” eddies showed maxima at different locations, apparently because a combination of strong thermal gradients with strong surface currents is needed for their manifestation in SAR imagery.

Moreover, the average daily numbers of eddies per unit area show a significant seasonal variability in the appearance of “black” eddies in SAR images, with highest numbers of eddies encountered during summer and autumn.

5. ACKNOWLEDGEMENTS

The authors are grateful to Frank Janssen and Thorger Brüning of the Bundesamt für Seeschifffahrt und Hydrographie (BSH), Hamburg, Germany, for making available the DWD model data.

6. REFERENCES

- [1] Alpers, W. and H. Hühnerfuss, “The damping of ocean waves by surface films: A new look at an old problem,” *J. Geophys. Res.*, 94, C5, 6251–6265, 1989.
- [2] DiGiacomo, P.M. and B. Holt, “Satellite observations of small coastal ocean eddies in the Southern California Bight,” *J. Geophys. Res.*, 106(C10), 22,521–22,543, doi:10.1029/2000JC000728, 2001.
- [3] Dokken, S.T. and T. Wahl, “Observations of spiral eddies along the Norwegian Coast in ERS SAR images,” *FFI Rapport 96/01463*, 1996.
- [4] Espedal, H.A., O.M. Johannessen, J.A. Johannessen, E. Dano, D. Lyzenga, and J.C. Knulst, “COASTWATCH ’95: A tandem ERS-1/2 SAR detection experiment of natural film on the ocean surface,” *J. Geophys. Res.*, 103, 24969–24982, 1998.
- [5] Gade, M., V. Byfield, S. Ermakov, O. Lavrova and L. Mitnik, “Slicks as Indicators for Marine Processes,” *Oceanography*, 26(2), 138–149, 2013.
- [6] Johannessen, J.A., R.A. Shuchman, G. Digranes, D.R. Lyzenga, C. Wackerman, O.M. Johannessen, and P.W. Vachon, “Coastal ocean fronts and eddies imaged with ERS-1 synthetic aperture radar,” *J. Geophys. Res.*, 101(C3), 6651–6667, doi:10.1029/95JC02962, 1996.
- [7] Karimova, S., “Spiral eddies in the Baltic, Black and Caspian seas as seen by satellite radar data,” *Adv. Space. Res.*, 50 (8): 1107–1124, 2012.
- [8] Karimova, S. and M. Gade, “Eddies in the Red Sea as seen by satellite SAR imagery,” In “*Remote Sensing of the African Seas*”, V. Barale and M. Gade (Eds.), Springer-Verlag, Berlin Heidelberg, pp. 357–378, 2014.
- [9] Karimova, S. and M. Gade, “Sub-mesoscale eddies seen by spaceborne radar,” *Proc. EMEC 10 – MEDCOAST 2013*, 30 Oct - 03 Nov 2013, Marmaris, Turkey; Dalyan, Mugla, Turkey, Vol. I., pp. 665–676, 2013.